Engineering Science and Technology, an International Journal 17 (2014) 73–84

Contents lists available at ScienceDirect

Engineering Science and Technology, an International Journal

journal homepage: http://ees.elsevier.com/jestch/default.asp

Full length article

Pipeline unplugging experiments with the Fluidic Wave-Action Technology

Seckin Gokaltun [a,*], Dwayne McDaniel [a], Amer Awwad [a], Jose Varona [b]

[a] Applied Research Center, Florida International University, 10555 W. Flagler ST, EC2100, Miami, FL 33174, USA
[b] University of Miami, 1535 Levante Avenue, Coral Gables, FL 33146, USA

ARTICLE INFO

Article history:
Received 12 December 2013
Received in revised form
26 March 2014
Accepted 27 March 2014
Available online 27 April 2014

Keywords:
Pipeline unplugging
Fluid transients
Method of characteristics
Wave erosion
Plug removal
Transfer lines
Nuclear waste

ABSTRACT

A 7.62-cm diameter pipeline network was built at Florida International University in order to facilitate data acquisition for design optimization and performance evaluation of a pipeline unplugging technology by NuVision Engineering that was based on the fluidic wave-erosion principle. Three types of plug materials were used at three different test bed lengths (86.87, 189.28, and 547.73 m) to determine the effectiveness of the technology with respect to pipeline length. Erosion rates were determined for each plug type and at each test bed length. Although some correlation was observed between erosion rates and other test parameters, the parameters that directly influenced it were not easily discernible. The unplugging technology was observed to create an amplification of pressure at the plug location which was correlated to the process control parameters (i.e. an increase in drive time for the same drive pressure will increase the amplification factor an increase in suction time will decrease the amplification factor). It was also noted that the cavity size affected the amplification factor and resulting wave speeds. A numerical method based on the Method of Characteristics was used to predict the pressure and flow rates generated by the fluid transients caused by unplugging technology in the pipe. It was found that the results obtained from the numerical model was in good agreement with the pressure variation measured in the pipeline and that the modeling can be used to predict unplugging performance at longer pipelines.

1. Introduction

The Department of Energy (DOE) Hanford Site is the world's first plutonium production complex which was active from 1944 to 1989. As a result of the nuclear weapons program 53 Mgal of radioactive waste was generated and stored in 177 underground tanks at Hanford. Since 1959, 67 of the 149 single-shell tanks built in the 40's to mid-60's are assumed to have leaked about 1 Mgal of liquid waste into the ground. DOE has started the Hanford clean-up effort in 1989 and is currently in the process of transferring the waste to double-shell tanks where no leakage has been detected so far. One of the challenges during this retrieval and disposal program is the formation of plugs during the cross-site pipeline transfers. In the past, some of the pipelines have plugged during waste transfers, resulting in schedule delays and increased costs [9,11,19]. Furthermore, pipeline plugging has been cited as one of the major issues that can result in unplanned outages at the Hanford Waste Treatment and Immobilization Plant (WTP), causing inconsistent operation [12]. As such, availability of a pipeline unplugging technology is crucial to ensure smooth operation of the waste transfers and to ensure Hanford tank farm cleanup milestones are met [5].

Florida International University (FIU) has previously tested and evaluated various unplugging technologies through an industry call that consisted of in-situ and remote mechanical methods for pipeline unplugging [2]. The in-situ methods utilized hydraulic pressurization and mechanical abrasion to unplug the line. One such method evaluated included technologies such as the Harben high-pressure jet system, which had a variety of jet heads that could be attached to a cleaning hose and operated between 6.89 and 27.58 MPa. The system used in the FIU testbed was also equipped with Harben's pump jet water pulsation module, which assisted the system in clearing difficult blockages as well as aiding the hose around obstacles such as elbows. The system was used in an open-ended pipeline to allow for the insertion of the cleaning hose and the drainage of the removed blockage material and water. The jet head was attached to the end of the hose and acted as both the propulsion system and the cleaning method. Another in-situ technology evaluated was the Aqua Miser, a 103.42–275.79-MPa water jet system. Due to the large pressure drop across the hose,

* Corresponding author.
E-mail addresses: gokaltun@fiu.edu, gokaltun@gmail.com (S. Gokaltun).
Peer review under responsibility of Karabuk University

http://dx.doi.org/10.1016/j.jestch.2014.03.005

the technology could only be extended to approximately 121.92-m straight run (or 76.20 m with elbows), limiting long-distances between plug and pipeline inlet. An additional in-situ method tested was the Ridgid Snake, which consisted of an approximately 45.72-m long semi-flexible steel rod with a cutting blade tip that is inserted into the pipeline for cleaning blockages. The snake was housed inside a rotating drum, which was used to feed and retract the snake from the pipeline. These in-situ methods were all capable of removing specific plug types, as long as the plugged location was at a short distance from a pipeline access point.

As many of the pipelines used to transfer high-level radioactive waste cannot be accessed without exposure to workers and equipment, innovative methods are needed that can remove blockages remotely and non-invasively. One such remote method involves the utilization of pressure pulses to remove fouling material or blockages in pipelines which has been documented in various patents [4,6,7] and research articles [13,15,23]. Mazzola et al. [13] used pulsed acoustic waves to remove biofouling material from the inner walls of pipes and heat exchangers while Paddock et al. [15] presented a horizontal wellbore cleaning method based on the generation of ultrasonic pressure waves. Zollinger and Carney [23] developed a hydraulic system that could create pressure pulses to resonate the water column and the pipe walls at different frequencies that results in the removal of blockages.

The remote methods tested at FIU utilized high-frequency pressure pulses or wave erosion to dynamically load the plug. One system evaluated was the Hydrokinetics Technology provided by AIMM Technologies. This system operated on the principle of repeated, high-frequency pressure pulses injected into pipeline, in order to create vibrations in the pipe wall and the plug at different frequencies. These mismatched oscillations aimed at dislodging the plug by breaking he bonds between the wall and the plug. Another system evaluated was NuVision Engineering's Fluidic Wave-Action Technology (FWT). The system operated much like the ocean wave-action on beach erosion, coupled with positive and negative pressure pulses that tend to loosen the blockage. It could operate on a long pipeline that has drained down below a blockage. Based on mockup testings at FIU, these technologies were identified as two alternative methods that could withstand the rigors of operation in a radioactive environment and had the ability to handle sharp 90° elbows. A separate assessment by Oak Ridge National Laboratory for the identification of commercially available unplugging methods confirmed these findings [14]. In this paper, the testing and data analysis of only the FWT are presented because the tests with the Hydrokinetics method have shown that the technology was not successful in unplugging the pipelines when they were made to operate within the pressure limit of the DOE transfer lines, 2.07 MPa.

The outline of this paper is as follows: First, the experimental set-up is presented and the operating principles of the FWT are described. Next the results of the data analysis are explained for the unplugging performance of the system. A mathematical model is presented to estimate the performance of the FTW in terms of pressure distribution in the pipeline during an unplugging event. Finally conclusions are drawn and some of the uncertainties in the results are discussed.

2. NuVision's unplugging technology

NuVision's FWT is based on fluid wave-action principles which can be used to oscillate a water column in the pipeline repetitively in order to loosen a blockage. It can operate on a long pipeline that has drained down below a blockage. The system consists of a water/solvent tank, a pressurize/vacuum vessel (charge vessel), a portable air compressor, jet pump pairs and valve manifold, a fluidic control unit, a vacuum finishing pump, a system controller, and a system module (Fig. 1). The pipeline unplugging operation principles of

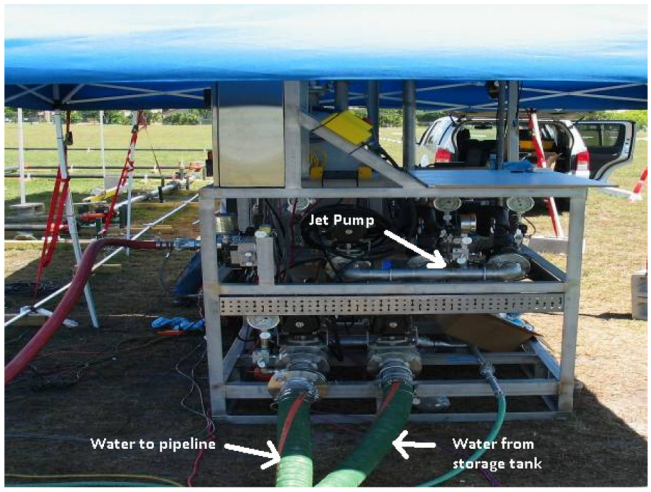

(a) front view

(b) side view

Fig. 1. Fluidic Wave-Action Technology pipeline unplugging skid.

Nuvision's FWT are as follows: First, a vacuum pump is used to evacuate a majority of the air in the pipeline below the blockage in elevation. Once the desired vacuum has been established, a ball valve is opened, and the fluid is allowed to back-fill the pipeline. Since a portion of the air remains in the pipeline, a cavity forms near the elevated blockage. The fluidic control system is then used to generate waves in the fluid by providing positive and negative pressures to the fluid in a cyclic manner.

A cycle consists of three phases: a suction phase, a drive phase and a vent phase. During the suction phase, some of the fluid in the pipeline is pulled back into the charge vessel. The fluid is quickly expelled during the drive phase, creating a wave in the cavity near the blockage. In the vent phase, the system is vented to the atmosphere, allowing the fluid to settle. This process is repeated numerous times until the blockage is removed.

The frequency and duration, as well as the pressure, of each cycle can be controlled via the fluidic control unit. This coupled with the dissolving action of a selected solvent and the physical action of the vacuum and pressure cycles works to both erode and loosen the blockage.

To create the fluidic-wave action, NuVision uses a complex pneumatic pumping system. Water is stored in a 3.79-m^3 storage tank and enters the pumping skid. Water can be allowed to flow

directly into the pipe test bed or it can be used to fill the 0.15-m^3 charge vessel. An air compressor provides compressed air at 0.97 MPa. The compressed air is passed through a jet pump which can provide a vacuum and pull water from the pipeline into the charge vessel (suction phase) or it can be used to provide a positive air pressure and drive the water from the charge vessel. Prior to flooding the pipeline, the jet pump is used to pull a vacuum in the pipeline. A vacuum pump is then used to achieve the vacuum level needed, with the magnitude of vacuum pulled dictating the size of the air cavity. With the low pressure established in the pipeline, the water storage tank is used to flood the pipeline until the pressure is stabilized.

After the pipeline is flooded, the equipment is used in a three-phase cycle that is continuously repeated to remove the blockage. Prior to operating the equipment, the equipment control parameters that need to be set are: vacuum level, drive pressure level, suction time, drive time and vent time (or vent pressure level).

3. Experimental set-up

The instrumented test bed for technology qualification was designed and constructed with the capability to evaluate the impact of a number of parameters on the technology effectiveness, including: the distance to the plug, pipe layout (e.g., bends, expansions, reducers, etc.) and connection with limited accessibility (through a Hanford connector inside a pit). Schematic diagrams of the test beds are shown in Fig. 2. The test beds were constructed using 7.62-cm diameter, 53.34-cm long, Schedule 10, carbon steel pipe sections joined by Victaulic couplings. To simulate the connection to the transfer lines in a pit, the inlet section was connected vertically to the long horizontal section via a sharp 90° elbow. The test bed entry point was equipped with a standard 7.62-cm flange (Victaulic 741). As shown in Fig. 2, pressure transducers were located throughout the test bed to evaluate the effects of pipeline length and configuration changes such as elbows, reducers and expansion joints. In addition, a number of pressure transducers were placed near the blockage.

Three 2.44-m clear PVC pipe sections were located upstream of the blockage as shown in Fig. 3. This allowed for the visual examination of the wave as it approached the blockage. The clear section was inclined at 1° to simulate the pipeline grade at the DOE Hanford site. The blockage was placed into a 1.22-m section of clear PVC. The low coefficient of friction between the PVC and some of the plugs required that a ball valve be placed just behind the blockage in order to prohibit the blockage from moving, without which, the blockage could have been pushed out during the testing process. A 53.34-cm pipe section was used as the discharge section and was placed after the ball valve. The operating pressure of the clear PVC was the test beds limiting component, with a maximum operating pressure of 1.034 MPa; therefore, a pressure relief valve, rated at 1.034 MPa, was installed upstream and adjacent to the clear inclined section. Also shown in Fig. 2, is a removable expansion joint located just upstream of the inclined clear section. This joint containing three 3.048-m sections, emulated the by-pass connections typical of the cross-site lines at Hanford (Fig. 4(a)). The expansion joint was removed in some of the cases to evaluate the effectiveness of the technology with and without the joint. Two removable reducers were used to create a sudden constriction in the pipeline diameter to 5.08 cm with a subsequent expansion back to 7.62 cm in order to evaluate its effects on the technologies effectiveness (Fig. 4(b)). The reducer was installed on the 86.87-m test bed, upstream of the expansion joint.

A total of 13 pressure transducers (Omega PX209) with a range of −101.35 to 930.79 kPa and 2 ms of response time were placed at

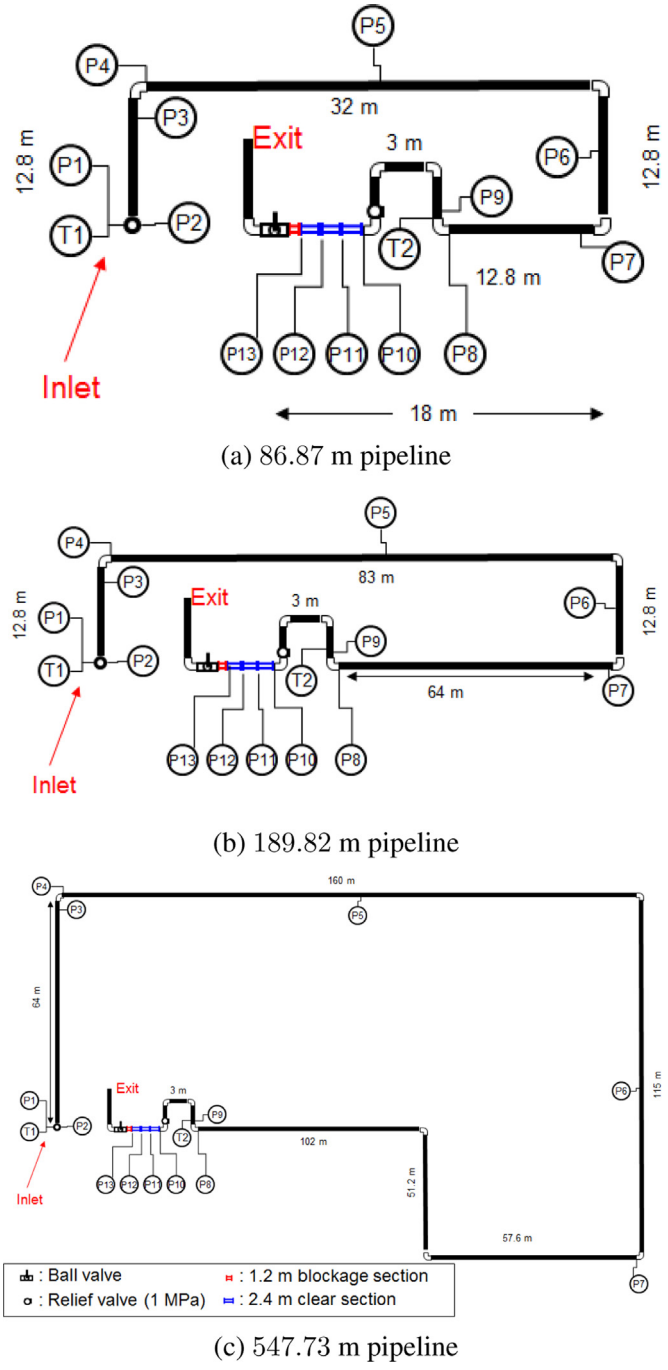

Fig. 2. Schematic of the test beds (Dimensions not to scale).

various locations along the pipeline in order to track the propagation of the pressure wave inside the pipeline. The transducers were connected to a National Instruments Field Point data acquisition system for simultaneous recording of pressure along the test bed during the unplugging tests.

3.1. Blockage materials

Three blockage materials were used in order to evaluate how the effectiveness of the unplugging technology was impacted by the chemical and rheological characteristics of the plug. A kaolin clay water mixture was used to emulate settled sludge while phosphate and aluminum gel type plug materials were used to emulate a

Fig. 3. 7.32-m inclined clear pipe sections of the pipeline used for visual observation.

crystallized salt plug. Literature suggests that the most relevant blockage material property with respect to conveyance system potential of plugging, choking, and slugging is cohesiveness [8,17]. Cohesiveness characterizes the tendency of the material to adhere to itself and to the conveyance system equipment. For many sludge-like materials, the expected cohesiveness is a function of the shear strength [17]. Kaolin clay water mixture was recommended as a sludge simulant by Golcar et al. [8] and Powell et al. [17] because its shear strength, cohesiveness, particle size distribution, and density (at 66–67 wt% kaolin in water) are similar to those of tank sludge (Table 1). Further information on kaolin clay simulants such as particle size distribution, shear strength and rheology data are available in the literature [16,17]. The authors of this paper also conducted shear strength, tensile strength, and stickiness measurements of kaolin clay water mixtures and verified that shear and tensile strength of kaolin-water mixtures used in this study were similar with literature (Fig. 5).

The kaolin-water mixture was prepared in a large bucket and mixed using a drill attachment until uniformity was achieved. Four-foot PVC pipes were then completely filled with the mixture. In order to remove air gaps that can get entrapped inside the blockage during filling, the blockages were compressed to 10.68 kN using a torque wrench.

Hanford and WTP engineers recommended that phosphate and aluminum gel be used as the crystallized salt blockage simulants. This type of plug may form in a pipeline due to precipitation of waste salts caused by temperature changes or supersaturation due to mixing of different waste types [10]. Composition of the phosphate simulant is given in Table 2 [18]. This composition was first prepared in small samples in the laboratory and it was observed to form a gel when cooled to room temperature. In order to get 1.22 m of the phosphate blockage, two batches of 0.003 m^3 of gel were prepared as shown in Fig. 6(a). The ends of the clear pipe were

Table 1
Comparison of material properties of Kaolin water mixture with those of Hanford tank sludge.

	$\overline{d}$ (μm)	τ_s (kPa)	ρ (g/cm^3)
Kaolin water mixture (66 wt%)	1.02	3.5	1.65
Tank sludge	1.2	0–5	1–2

closed and the gel was poured into the pipe until full. It was left to drain in an upright position and new gel was added from the top as the water drained from the pipe (Fig. 6(b)). This process was repeated until water no longer drained from the pipe, which took approximately 5–7 days.

The recipe for the aluminum gel was provided by WTP and the Pacific Northwest National Laboratory (PNNL) which required preparing a matrix solution and a gelling solution separately. Beaker testing was performed and gelling was observed (Fig. 7). First, the aluminum nitrate was dissolved in water separately to prepare the matrix solution. Sodium hydroxide and sodium carbonate were dissolved in a separate cup to prepare the gelling solution. Finally, the gelling solution was added to the matrix solution to get the final Al–OH gel. The compositions of the ingredients are given in Table 2. A draining procedure similar to phosphate gel was carried out for the Al-gel blockage. A hand plunger was used to increase the mechanical integrity of the blockage.

All of the plugs were created in 1.22-m pipe lengths. They were weighed before and after each unplugging test to determine the weight of removed plug material and effective unplugging rates.

3.2. Test plan

Table 3 summarizes the parametric test plan that included sixteen trials with three different blockages used at each of the three pipeline lengths. Only erosion and dissolution methods are considered for unplugging although unplugging the blockage with mechanical wave energy was also possible.

An expansion joint was used in the baseline test bed for all blockage types and all pipe lengths, whereas one trial was conducted at each pipeline length without the expansion joint using a kaolin blockage to determine the effects of the expansion joint on the unplugging rates (marked in Table 3 as NEJ). For the 86.87-m test bed, a constriction was inserted using two 7.62 cm–5.08 cm reducers just upstream of the expansion joint to see what effects it may have on the pipeline pressures and unplugging rates. In addition, blind flange testing (no plug) was conducted in which the drive pressures, drive times and suction times were varied to analyze their effects on the wave mechanics and resulting pressures.

(a) Expansion joint before the clear section. (b) 7.62 − cm to 5.08-cm reducers.

Fig. 4. Expansion joints and reduction in pipe cross-sectional area was also evaluated.

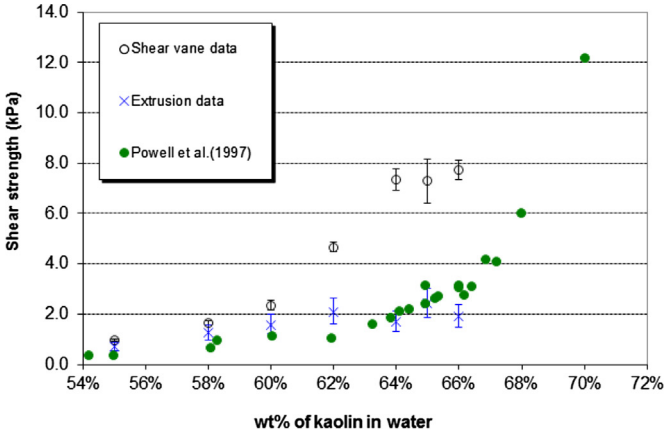

(a)

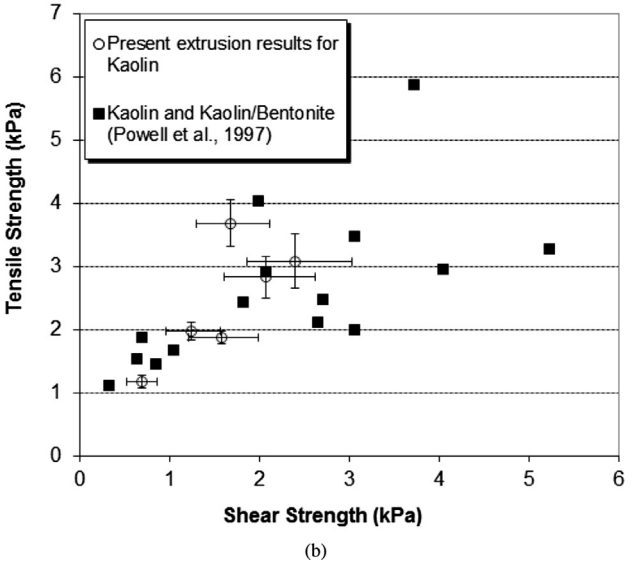

(b)

Fig. 5. Physical properties of kaolin-water mixture used in this study.

It should also be noted that some of the early tests were run with the charge vessel empty. This potentially resulted in adding air into the pipeline during the drive phase and ultimately required changes in the control parameters during testing. These tests were rerun with a partially filled charge vessel with the exception of the phosphate tests since the phosphate plugs seemed to dissolve relatively easily in the presence of water. The cases with an asterisk in Table 3 indicate that these tests were conducted without a partially filled charge vessel.

In general, NuVision varied three of the five equipment control parameters: suction time (T_s), drive time (T_d) and drive pressure (P_d). Vent time (T_v) was initially set to a specific time but after a few tests it was set to a specific level of pressure ($P_v \sim 20$ kPa). The vacuum level (P_{vac}) was generally fixed except the 547.73 m test bed where higher levels of vacuum were pulled to reduce the cavity size. Separate blind flange testing was also conducted at each pipe length, varying drive pressure, drive time and suction time in order to determine the effects of each of the equipment control parameters on the wave and pressure dynamics without the influence of the blockages. A key observation from Table 3 relates to the variation in the equipment control parameters. As the pipe length test bed increases, the variability in the control parameters utilized also increases. This is believed to be due to the ambient environmental variations observed during testing which affected the cavity size and ultimately the performance of the technology.

Table 2
Molarity values of chemicals in Phosphate and Aluminum blockage simulants.

Component	Phosphate	Aluminum
$NaAlO_2$	1.0	0.0
NaOH	2.0	3.0
Na_2CO_3	0.1	0.5
$NaNO_3$	7.0	0.0
$Na_3PO_4 0.25H_2O 12H_2O$	0.3	0.0
$Al(NO_3)9H_2O$	0.0	1.0

4. Experimental results

4.1. Pressure profile in the pipeline

During the erosion process, the drive pressure added momentum to the column of fluid in the pipe which had two effects; 1) it compressed the air remaining in the cavity causing an increase in pressure at the blockage location and 2) created a wave which in turn attempted to erode the blockage. The increase in pressure can sometimes result in the amplification of pressure at the location of the plug compared to the drive pressure as shown in Fig. 8. Understanding this amplification of the pressure is one of the key concepts in qualifying NuVisions technology for safe deployment at DOE transfer lines. It was observed that the amplification factor ($G_i = P_{plug}/P_{inlet} = P_{13}/P_1$) may vary even when the control parameters were kept same over a number of cycles with the same drive pressure. In order to get the mean amplification factor ($\overline{G}$) the observed amplification factors were averaged by $\overline{G} = \sum_{i=1}^{N} G_i/N$ where N is the total number of cycles.

Three main process control parameters (T_d, T_s and P_d) were varied to determine their effects on the $\overline{G}$. Initially a blind flange was used instead of a plug to eliminate any effect of the blockage material on the $\overline{G}$. Fig. 9 shows the variation of $\overline{G}$ with respect to T_d for fixed values of P_d and T_s whereas a similar relation of $\overline{G}$ versus T_s is given in Fig. 10. In general, it was observed that for fixed T_s and P_d, increasing T_d resulted in an increase in the $\overline{G}$. This can be explained by the fact that T_d and T_s determine the amount of water injected into the pipeline. If the amount of water introduced during the drive phase was increased, i.e. a longer drive period, the air bubble was compressed more which increased the pressure of the air cavity and the $\overline{G}$. For this scenario, it would be expected that a point would be reached where the increase in drive time would cease to compress the air cavity and would only result in a loss in energy.

The opposite is observed for T_s. For increasing T_s the amplification factor was seen to decrease almost linearly as shown in Fig. 10. As the suction duration increased and the T_d was kept constant, the volume of the fluid in the pipeline being cycled reduced which increased the volume of the air cavity at the pipe end. This resulted in a reduction in $\overline{G}$ since the water left in the pipeline was not able to compress the same volume of air as it could with a lower value of T_s.

Figs. 9 and 10 show that in general, the drive pressure works in favor of the amplification factor. For all of the pipelines, the general trend showed that for the same T_d and T_s, an increase in the P_d assigned by the NuVision engineers yielded in an increase in the $\overline{G}$. A larger P_d corresponded to a higher piston force in the charge vessel which increased the energy input into the system for constant T_d and T_s and resulted in higher wave velocities hitting the blockage. As a result, the net momentum compressing the air cavity was increased with an increase in P_d which resulted in larger $\overline{G}$ values.

(a) Phosphate plug prepared in batches (b) Draining process

Fig. 6. Preparation of the 1.22-m Phosphate plug.

4.1.1. Pressure amplification for cases with blockages

In Figs. 9 and 10 the $\overline{G}$ values obtained with blockages in the pipeline are represented with symbols for each of the three test bed lengths. These plots provide the effects the blockages may have had on the amplification factors that were obtained. In Fig. 9(a) the kaolin and aluminum gel trials appear to be in line with the blind flange results, for the 86.87 test bed. Note that the variance for each run has also been provided in the figure. The phosphate trial has a large variance which was due to the testing without a pre-charged vessel. Although the average drive time appears to be similar to the amplification factor for the $T_d = 5$ s, the data for $T_s = 15$ s does not have a corresponding trend line on the figure. The kaolin trial without the expansion joint is also shown at a $T_d = 4$ s with a significantly larger $\overline{G}$, as expected.

Although the suction times for the blockage cases for the 189.28 m test bed shown in Fig. 9(b), lies outside of the trend line, the variance of the phosphate and the kaolin encompass the amplification factor trend line. In addition, the kaolin trial without the expansion joint again is significantly higher for the same suction time ($T_s = 8$ s) at $T_d = 4$ s. For the 547.73 m case, the variance of the process control parameters from plug-to-plug make it difficult to determine any correspondence between the plug data and the blind flange data.

Fig. 10 shows similar plots with suction time replacing the drive time on the *x*-axis. It was observed that the kaolin and aluminum gel trials match well with the corresponding trend lines in the 86.87 m test bed. The kaolin trial without the expansion joint again appears to be significantly higher than the extrapolated trend line. For the 189.28 m test bed, there appears to be more scatter in the data with the exception of the kaolin trial without the expansion joint which corresponds well with the $T_d = 7$ s trend line even though the $T_d = 4$ s for that trial. For the 547.73 m test bed, variations in the process control parameters made it difficult to access any correlation between the two sets of data.

Fig. 7. Aluminum gel after beaker tests.

4.2. Unplugging rates

Table 4 presents the unplugging rates that are obtained by calculating the difference between the initial and final weights of

Table 3
Text matrix and plug removal rates. All cases used vent pressure ($P_v = 20$ kPa) except the Phosphate blockage cases at 86.87 m ($T_s = 1$ s) and at 547.73 m ($P_v = 20$ kPa or $T_s = 8$ s whichever first achieved).

L(m)	Blockage	T_s(s)	T_d(s)	T_v(s)	P_v (kPa)	P_d(kPa)	P_{vac}(kPa)	$\dot{m}$(Kg/h)
86.87	Kaolin	11	6	–	20	200	−8.86	0.452
86.87	Aluminum	11	6	–	20	200	−8.86	0.704
86.87	Phosphate*	15	5	1	–	200	−8.85	9.5
86.87	Kaolin (NEJ)	8	4	–	20	200	−8.89	0.9
189.28	Kaolin	14	6	–	20	300	−8.86	0.650
189.28	Aluminum	18	7	–	20	300	−8.80	0.477
189.28	Phosphate*	15	7	–	20	300	−8.80	10.31
189.28	Kaolin (NEJ)	8	4	–	20	300	−8.80	0.282
547.73	Kaolin	17	8–10	–	20	300	−8.80	0.214
547.73	Aluminum	14–16	7–9	–	20	150–200	−9.16	0.146
547.73	Phosphate*	15–16	7–10	8	20	150–250	−9.28	6.332
547.73	Kaolin (NEJ)	17	11	–	20	200	−9.28	0.088*

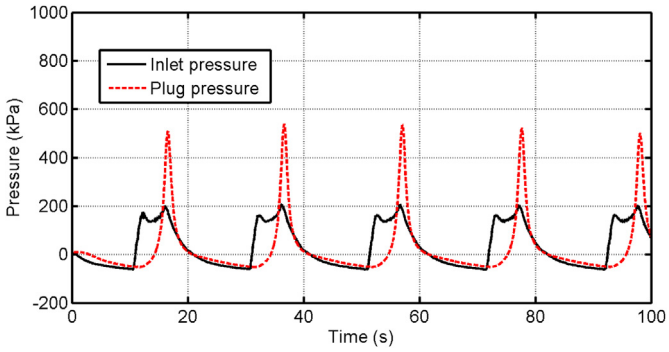

Fig. 8. Pressure amplification in the 86.87-m pipeline (P_d = 172.37 kPa, AF = 3).

the pipe section containing the blockage material over the total time of unplugging spent on the blockage. Blockages were typically eroded between 25 and 50% of the original mass with the exception of the phosphate blockage which was completely dissolved at each test bed length. In general, the unplugging rates obtained with the aluminum gel blockages were similar to those obtained with the kaolin blockages. The trials without the expansion joints were unpredictable. For the 86.87 m test bed, the unplugging rate of the kaolin was significantly higher when the joint was removed. This was not the case for the longer runs. In the 547.73 m trial without the expansion joint, an extremely low rate was observed (* in Table 4). This was due, in part, to the fact that the kaolin near the wave did not erode easily, but water did manage to penetrate into the plug. When weighing the blockage to determine the percentage of erosion, the additional water retained by the plug may have skewed the final calculated rate, indicating a less effective unplugging rate than what actually occurred. Unplugging rates for the longest pipeline length were lower than the rates for the other two lengths, as expected. However, there was not a pattern for the unplugging rates between the 86.87 m and 189.28 m test beds. It should also be noted that during the 547.73 m trials, the process control parameters were varied over the erosion process. Although altering the parameters would affect the unplugging rate, the average unplugging rates are still presented. Note that the phosphate plug data is included in Table 4 but these trials were conducted without a pre-filled charge vessel.

One should expect that as the length of the testbed increases, the erosion rates would reduce. This is seen for all cases except for the kaolin and phosphate plugs when comparing the 86.87 m and 189.28 m testbeds. In terms of the phosphate, the erosion/dissolving process was simply dependent on the volume of fluid the wave deposited on the face of the plug, not the impact of the wave. For these two testbed lengths, the erosion rates were similar, so this is not surprising. The kaolin plug did have a slightly higher erosion rate and this is likely due to the variability obtained in the shear strength of the kaolin mix as well as how much air remained in the plug at the time it was manufactured.

4.3. Effects of reducer and the expansion joint

Table 5 shows $\overline{G}$ values obtained for blind flange tests at the 86.87 m pipeline with and without the reducer. It was found that the tests with the reducer resulted in a 9–19% reduction in the amplification factor when compared with cases run without the reducer installed. Table 5 shows that for the same T_d and T_s, a higher P_d resulted in a larger loss in the $\overline{G}$. Reducing the T_d while keeping the T_s and P_d constant, the loss in amplification factor increased. However, reducing the T_s while maintaining a constant T_d and P_d reduced the effect of the reducer.

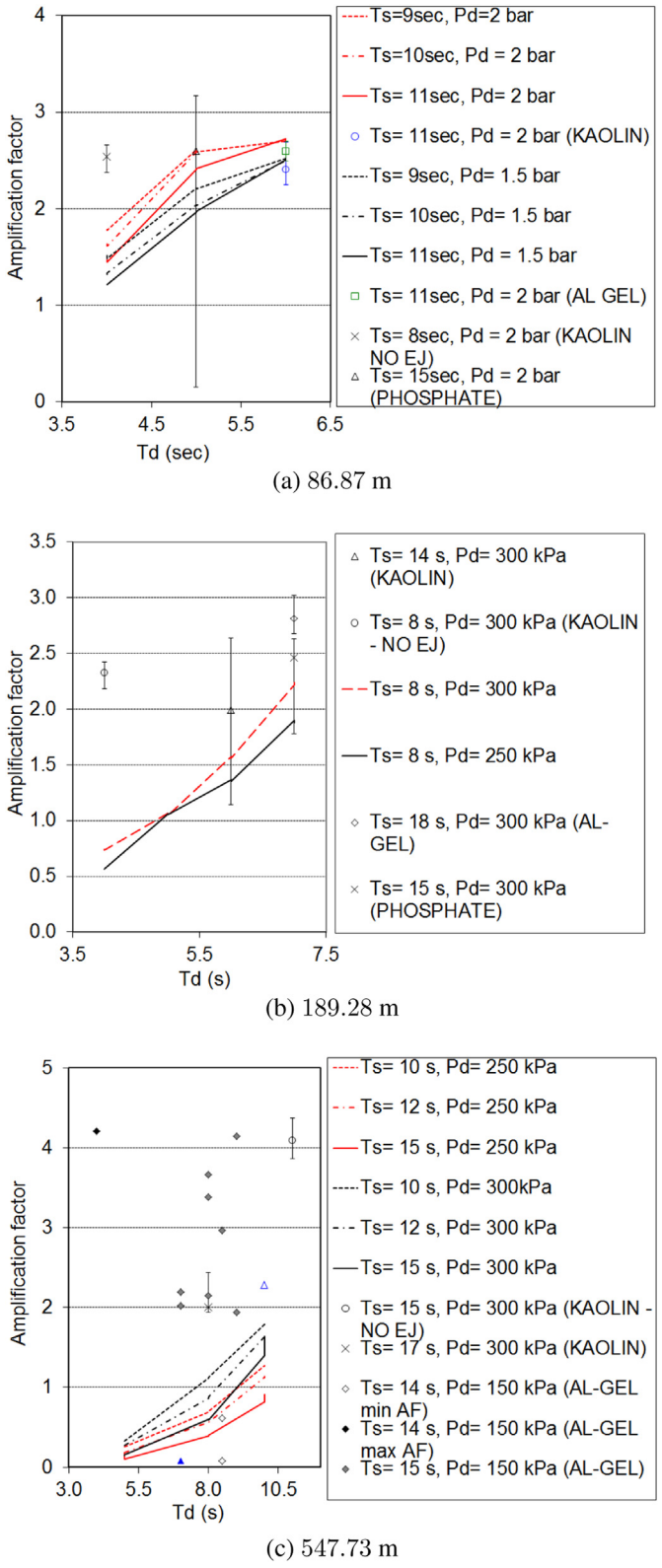

Fig. 9. Effect of the drive time on the amplification factor at various pipeline lengths (Line plots represent the blind flange data).

The unplugging rates with and without the expansion joints were unpredictable (Table 4). For the 86.87 m test bed, the unplugging rate of the kaolin was significantly higher when the joint was removed. This was not the case for the longer runs. In the

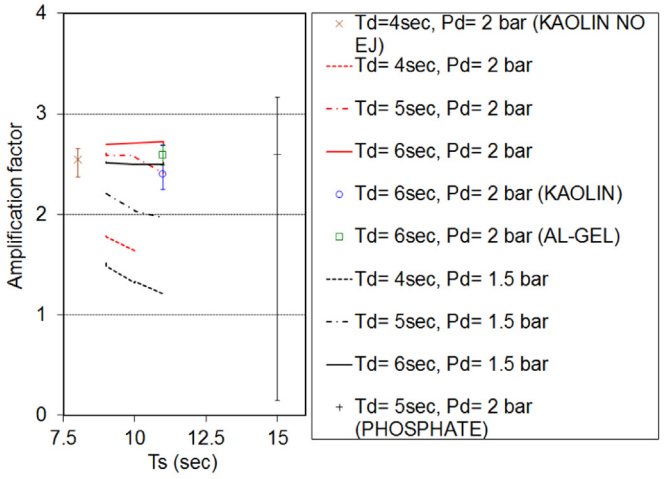

(a) 86.87 m

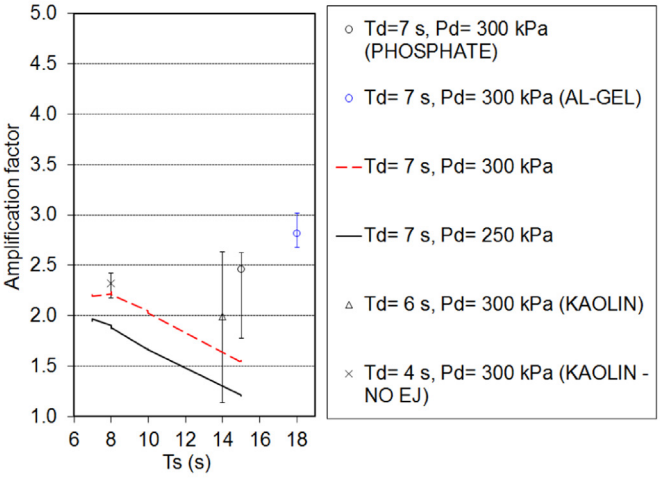

(b) 189.28 m

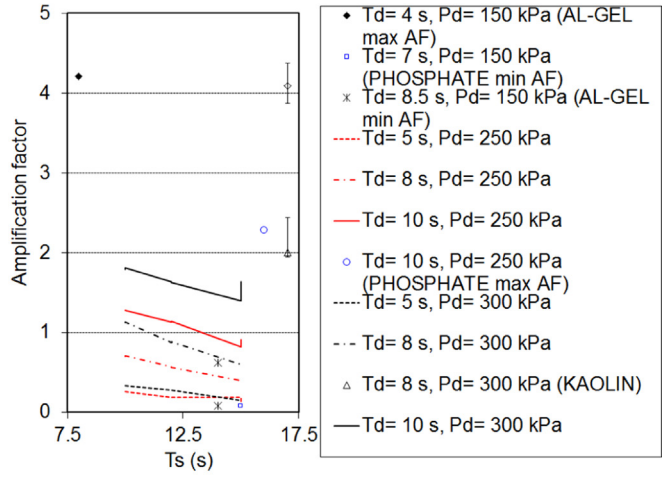

(c) 547.73 m

Fig. 10. Effect of the suction time on the amplification factor at various pipeline lengths (Line plots represent the blind flange data).

Table 4
Unplugging rates (kg/h).

	86.87 m	189.28 m	547.73 m
Kaolin	0.452	0.650	0.214
Phosphate	9.5	10.31	6.332
Aluminum	0.704	0.477	0.146
Kaolin (NEJ)	0.9	0.282	0.088*

547.73 m trial without the expansion joint installed, an extremely low rate was observed. This was due, in part, to the fact that the portion of kaolin plug near the wave did not erode easily, but water did manage to penetrate into the plug.

5. Numerical modeling

In this section, a numerical method based on the method of characteristics [22] that can predict the pressure and flow velocity in a straight one-dimensional pipeline with an air pocket at the end is presented. The aim of this effort was to predict the maximum pressures attained at any location in the pipeline caused by the operation of the unplugging technology so that parametric tests could be performed for much longer pipelines for which conducting experiments would not difficult. The numerical solution of the governing equations for unsteady fluid flow in pipelines consists of the following steps:

- Transformation of the partial differential equations (PDE) into ordinary differential equations (ODE),
- Integration of ordinary differential equations to yield finite difference equations,
- Numerical solution of the finite difference equations.

5.1. Governing equations

The continuity and momentum equations given below govern the unsteady fluid flow in a pipeline

$$H_t + \frac{a^2}{g} V_x = 0$$
$$gH_x + \frac{f}{2D} V|V| = 0 \quad (1)$$

where H is the hydraulic-grade-line elevation, a is the speed of sound, g is the gravitational acceleration, V is the flow velocity, f is the friction factor and D is the pipe diameter. These equations form a pair of quasi-linear hyperbolic partial differential equations, where velocity and hydraulic-grade-line elevation are the dependent variables and distance along the pipe and time are the independent variables. In order to convert this PDE to a more amenable

Table 5
Effect of reducer on the pressure amplification.

P_d(kPa)	T_s(s)	T_d(s)	$\overline{G}$ with reducer	$\overline{G}$ without reducer	% change
200	10	5	2.11	2.58	17.97%
200	11	6	2.34	2.70	13.22%
200	9	6	2.40	2.69	10.95%
200	9	4	1.43	1.78	19.49%
150	10	5	1.81	2.04	11.14%
150	11	6	2.20	2.50	12.13%
150	9	6	2.29	2.52	8.98%
150	9	4	1.23	1.50	17.97%

ODE, the equations are combined linearly using an unknown multiplier λ.

$$\lambda\left[H_x\frac{g}{\lambda}+H_t\right]+\left[V_t+V_x\lambda\frac{a^2}{g}\right]+\frac{f}{2D}V\left|V\right|=0 \tag{2}$$

Since H and V are dependent on x and t, and if it is assumed that x is also a function of t, then the equation may be written as

$$\begin{aligned}\frac{dH}{dt}&=H_x\frac{dx}{dt}+H_t\\ \frac{dV}{dt}&=V_x\frac{dx}{dt}+V_t\end{aligned} \tag{3}$$

If in the combined equation, the following relation holds, $dx/dt=g/\lambda=\lambda a^2/g$, then it can be written as

$$\lambda\left[\frac{dH}{dt}\right]+\left[\frac{dV}{dt}\right]+\frac{f}{2D}V\left|V\right|=0 \tag{4}$$

The solution of $dx/dt=g/\lambda=\lambda a^2/g$ gives two particular values of λ, which are $\lambda_1=g/a$ and $\lambda_2=-g/a$, which in turn yields that $dx/dt=\pm a$. This suggest that the change in position of a wave is related to the change in time by the wave propagation velocity a. When the values of $\lambda_1=g/a$ and $\lambda_2=-g/a$ are substituted into the above equation then two pairs of ODEs are obtained which are grouped and identified as C^+ and C^- as given below:

$$\left.\begin{aligned}+\frac{g}{a}\frac{dH}{dt}+\frac{dV}{dt}+\frac{f}{2D}V\left|V\right|&=0\\ \frac{dx}{dt}&=+a\end{aligned}\right\}C^+, \tag{5}$$

$$\left.\begin{aligned}-\frac{g}{a}\frac{dH}{dt}+\frac{dV}{dt}+\frac{f}{2D}V\left|V\right|&=0\\ \frac{dx}{dt}&=-a\end{aligned}\right\}C^-, \tag{6}$$

Since a is a constant for a given pipe, $dx/dt=a$ gives a straight line in the xt plane as shown in Fig. 11. Each straight line connecting A to P and B to P are the characteristic lines along which the information is carried from A and B to solve for the value at point P which is at the new time level. C^+ which is valid on A–P and C^- which is valid on B–P are used together in order to solve the future value at P.

5.2. Finite difference forms of the ODE's

In order to solve the above equations numerically, a pipeline is divided into N equal segments, each Δx in length as shown in Fig. 11.

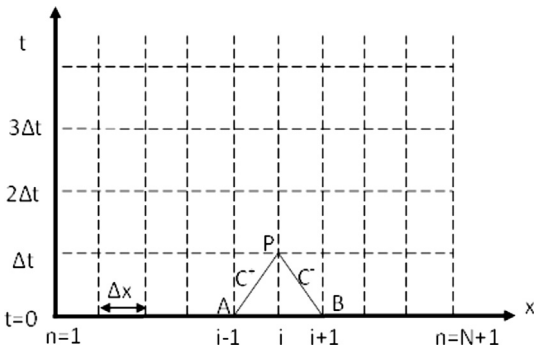

Fig. 11. xt grid for numerical solution of the pipe flow.

By using the initial values of V and H at $t=0$ at point A and point B, the compatibility equations can be integrated between the limits A–P and B–P. It becomes easier to integrate once the compatibility equations are multiplied by $a\,dt/g=dx/g$ and introducing the area of the pipe to write the equations in terms of discharge in place of velocity. The integrated from A to P becomes

$$\int_{H_A}^{H_P}dH+\frac{a}{gA}\int_{Q_A}^{Q_P}dQ+\frac{f}{2gDA^2}\int_{x_A}^{x_P}Q|Q|dx=0. \tag{7}$$

The integration along the characteristics results in the following algebraic equations

$$\begin{aligned}H_P-H_A+\frac{a}{gA}(Q_P-Q_A)+\frac{f}{2gDA^2}Q_A\left|Q_A\right|&=0,\\ H_P-H_B+\frac{a}{gA}(Q_P-Q_B)+\frac{f}{2gDA^2}Q_B\left|Q_B\right|&=0.\end{aligned} \tag{8}$$

Solving for H_P these equations may be written as

$$\begin{aligned}H_P&=H_A-B(Q_P-Q_A)+RQ_A|Q_A|,\\ H_P&=H_B+B(Q_P-Q_B)+RQ_B|Q_B|,\end{aligned} \tag{9}$$

where $B=a/gA$. The solution of transient fluid flow begins with steady state conditions for H and Q at $t=0$. Then the unknown H and Q values are found at each grid point along the pipe axial direction along $t=\Delta t$ then proceeding to $t=2\Delta t$ until the desired time duration has been reached.

5.3. Boundary conditions

The computational model used in this study was for a straight pipe having a closed end with an air pocket connected to a reservoir at the inlet as shown in Fig. 12. The total length of the pipe and the size of the cavity were varied according to the experimental case that was aimed to be compared with. In the numerical solution of this problem, the conditions at the ends of the pipeline played an important role which determined the boundary conditions to be used. For the upstream boundary condition, the unplugging technology creates a change in pressure using the jet-pump and the charge vessel. This effect in the numerical code was interpreted as a time-dependent function of hydraulic-grade-line $H_r=H_r(t)$. This time-dependent profile was obtained from the pressure transducer measurements recorded at the inlet of the pipeline. Once the H value at the first node was known, then Q value was determined by a direct solution of the C^- at the first node, $Q_P=(H_r-C_M)/B$ where $C_M=H_B-BQ_B+RQ_B|Q_B|$.

At the downstream, the air cavity was modeled as a lumped mass, where the pressure at any instant was assumed the same throughout the volume. The gas was assumed to follow the reversible polytropic relation $H_AV^n=C$ in which H_A is the absolute head equal to the gauge plus barometric pressure heads and V^n is the gas volume, where n is the polytropic exponent ($1<n<1.4, 1.2$ used here) and C is a constant. This relation between pressure and volume of the air cavity was introduced into the numerical solution by the equation,

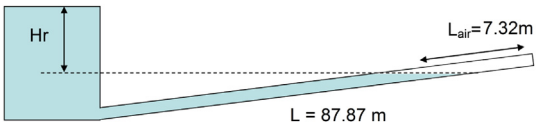

Fig. 12. Schematic of the unsteady pipe flow problem solved numerically.

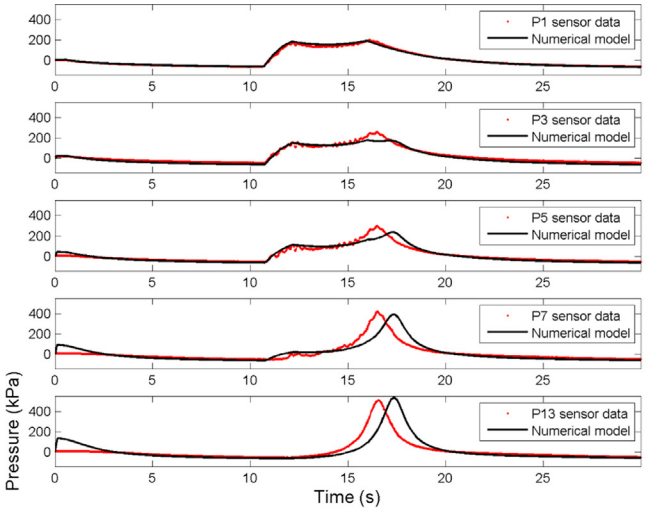

(a) 86.87 m, $T_s = 10$ s, $T_d = 5$ s, $P_v = 20$ kPa, $\Delta x = 0.87$ m, $\Delta t = 6.16 \times 10^{-4}$ s.

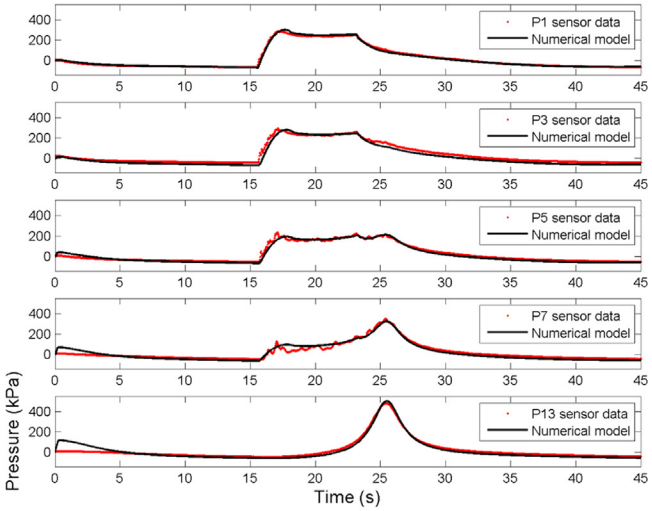

(b) 189.28 m, $T_s = 15$ s, $T_d = 7$ s, $P_v = 20$ kPa, $\Delta x = 3.8$ m, $\Delta t = 2.67 \times 10^{-3}$ s.

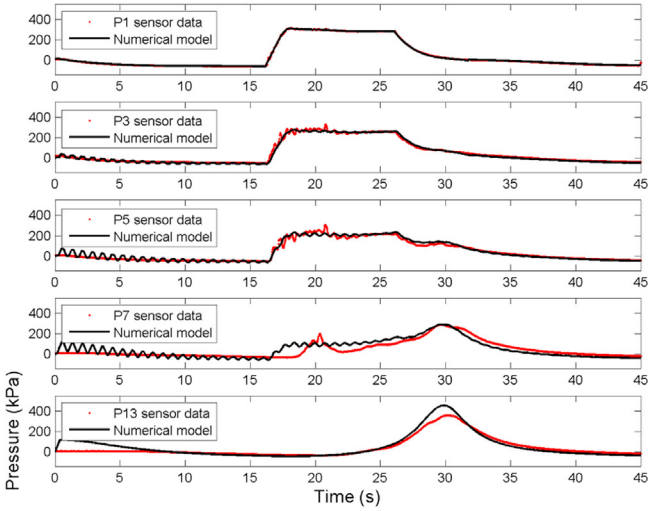

(c) 547.73 m, $T_s = 15$ s, $T_d = 10$ s, $P_v = 20$ kPa, $\Delta x = 2.62$ m, $\Delta t = 1.84 \times 10^{-3}$ s.

$$H_P\left(V_a - \Delta t\frac{(Q_P + Q)}{2}\right)^n = C. \tag{10}$$

The effects of elbows were not considered since for rigidly supported elbows the attenuation of pressure waves were reported to be negligible in the literature [20,21]. The total length specified in the numerical model consisted of all the components of the pipeline including the elbows, the expansion joint and the clear PVC section. The friction coefficient used in this work was $f = 0.02$. The value of the friction-factor was obtained from the Moody diagram for a relative roughness of 0.001 for 7.62 cm steel pipes with 7.62×10^{-3} cm of surface roughness which is constant over the fully turbulent regime. The air cavity at the end was modeled as a lumped mass whose axial location was fixed at the last point in the computational grid. The incoming flow rates were computed from the fluid region and this was used to calculate the pressure in the air cavity using the polytropic relation given above. This pressure value in turn was reintroduced into the fluid region as an end boundary condition.

Although not used in the current study, the method of characteristics allows to incorporate the effects of local elements in to the model. The simplest way to achieve this is possible by conserving the continuity equation at each time instant at the location of the connections and by assuming that the pressure at the connection is equal with minor losses ignored. In the case of serially connecting elements such as a reducer or a section with different structural properties such as thickness or roughness, the assumption of equal discharge and pressure at the connection yields $Q_P = C_P - C_M/B_1 + B_2$ from which H_P can also be calculated. In the case of a branching connection such as joints and turns, the same procedure is followed for the continuity equation with minor losses ignored and the solution for the common head H_P is obtained as $H_P = \sum_i^n (C_{P_i}/B_i)/\sum_i^n (1/B_i)$ for a connection with n number of branching.

5.4. Simulation results

Fig. 13 shows the pressure distribution along the pipelines obtained with the numerical method presented above. The blind flange data collected at all three pipelines was used to obtain the inlet pressure profile (P1) as a function of time, which was used as the upstream boundary condition in the numerical model. Only the first suction-drive-vent-suction cycle was modeled in the code. The cycle for 86.87 m pipeline started with 10 s of suction and then the water in the charge vessel was driven down for 5 s which is followed with venting the pipe until 20 kPa and the next suction phase is started again for 10 s. The initial air cavity length was taken as 3.96 m. The local pressure at various locations along the pipeline are shown in Fig. 13 where the red dots indicate the experimental measurements and the black lines are for the simulation results. The simulation result over predicted the maximum pressure by 1% and an offset in the location of the peak was observed.

For the case at 189.28 m, the control parameters were changed to 15 s for suction, 7 s for drive and 20 kPa for vent. The air cavity size increased to 53.34 cm. Simulation results matched the pressure data from the transducers perfectly at data acquisition points along the pipe. For the blockage distance of 547.73 m, the drive phase was 3 s longer than the 189.28 m case. The overshoot in the maximum pressure numerically computed at the cavity was 40%. However the pressure values obtained with the numerical code were found to be

Fig. 13. Comparison of the instantaneous pressure measurements from the blind flange experiments with the simulation results.

in good agreement with the experimental data at the locations far from the end of the pipeline such as P3 and P5.

6. Discussion

During the testing, a number of observations were made that would provide assistance in determining how the data can be used for assessing the effectiveness of the FWT in an unplugging operation at the Hanford Site. The amplification of the drive pressure near the blockage appeared to be due to the increased momentum of the fluid in the pipeline. If the drive pressure/drive time was too low, losses in the pipeline would decrease the momentum of the column of fluid to the point that a wave wouldn't be produced in the air cavity and there would be little amplification of the drive pressure. If the drive pressure/time would be too high, the resulting exit pressure could easily surpass pressure rating of the relief valve. Therefore, an optimization of the inlet operating conditions is required to generate the most adequate pressure rise in the system for safe and proper operation of the technology.

During the suction phase of each of the test beds, the air cavity was pulled back into the expansion joint, which was relatively flat. This suggests that the two-phase flow region in our test bed was larger than would be present on the cross-site lines at Hanford, therefore the energy losses of the unplugging wave were likely be more significant on our test bed.

Testing demonstrated that under the initial vacuum process, some blockages were pulled apart with portions being slightly moved upstream. The kaolin blockages were particularly susceptible to this due to the low coefficient of friction between the kaolin and the clear PVC. Typically, the blockage would break into two or three sections and the most forward section would move about a foot upstream. In some cases, the portion of the blockage that moved upstream would move back to its original position after the first drive phase.

In addition, testing also demonstrated that environmental conditions could have significant effects on test results. On the longer test bed lengths, the identical vacuums pulled on the pipeline did not necessarily produce the same cavity size. This required an unexpected change in the equipment system parameters. The environmental effects on the system's performance will likely require further investigation.

7. Conclusions

The objective of this study was to evaluate NuVisions unplugging technology for use at DOE Hanford transfer lines in the case of a pipeline plugging event. Experimental testing was conducted using three pipeline lengths and three types of blockages. An amplification of the inlet pressure was observed along the pipeline and is considered the key to determining the maximum pipe lengths the technology can be used without surpassing the site pressure limit.

The technology was capable of eroding the three plugs at the three test bed lengths and the results suggest that erosion of blockages located at greater lengths is also achievable. However, it is inconclusive on whether this technology can unplug a pipeline 5.79 km in length which was suggested to be a worst case scenario by the DOE engineers. Technology modifications will likely be required to meet the energy requirements for moving a column of water of that distance. Improved vacuum pump capabilities, and a larger charge vessel would be a necessity at larger pipe lengths. Other scenarios that this technology has proven to be useful are pulsed-jet mixing of slurries stored in DOE waste tanks [3] and feeding the liquid waste into delivery lines using reverse flow diverters [1]. In addition, it was found that the numerical method presented in this paper was capable of predicting the pressure variations in the pipeline caused by the technology which could be used for optimization of the process control parameters selection via a process simulation that may improve the ability to accurately predict maximum pressures and erosion rates.

Acknowledgments

The authors acknowledge Erich Keszler from Nuvision Engineering for providing technical information regarding the operation of the FWT. Funding for this work was provided by Department of Energy Environmental Management Office under grant No. DE-FG01-05EW07033.

References

[1] Fluidic Sampler, 1999. Report No. PNWD-3054, Tanks Focus Area.
[2] M. Allen, K. Coupet, A. Ebadian, P. Gibbons, F. Erian, M. Rinker, Evaluation of current technologies for mitigating blocked slurry pipelines, in: Proceedings of the 15th International Symposium on Hydrotransport, Banff, Canada, 2002, pp. 477–495.
[3] J. Bontha, N. Hannigan, Demonstration and optimization of bnfl's pulsed jet mixing and rfd sampling system using ncaw simulant, in: Proceedings of the Waste Management'01 Conference, Tucson, AZ, 2001.
[4] J. Coon and E. Petry. 1985. Vibration Method for Unplugging a Slurry Pipeline. US Patent 4,551,041.
[5] M. Corradini, D. Campbell, M. Draye, C. Drummond III, P. Hayward, L. Hobbs, E. Lahoda, R. Rogers, B. Sternberg, E. Zebroski, Research Needs for High-level Waste Stored in Tanks and Bins at U.S. Department of Energy Sites: Environmental Management Science Program, National Academy Press, Washington, DC, 2001.
[6] P. Garcia. 1997. Method and apparatus for cleaning columns by inducing vibrations in fouling material and the column. US Patent 5,674,323.
[7] R. Garcia. 1995. Method for Cleaning Heat Exchanger Tubes by Creating Shock Wave and Mixing the Liquid with Injected Air. US Patent 5,423,917.
[8] G. Golcar, J. Bontha, J. Darab, "Retrieval Process Development and Enhancements Project Fiscal Year 1995: Simulant Development Technology Task Progress Report, Report no., Pacific Northwest Lab., Richland, WA, 1997
[9] R. Hunt, T. Dillow, J. Parrott, J. Schryver, C. Weber, T. Welch, Waste Preparation and Transport Chemistry: Results of the FY 2000 Studies, Report No. ORNL/TM-2000/298, Oak Ridge National Laboratory, Oak Ridge, Tennessee, 1999.
[10] R. Hunt, T. Dillow, J. Parrott Jr., J. Schryver, C. Weber, T. Welch, Waste Preparation and Transport Chemistry: Results of the FY 2002 Studies, Oak Ridge National Laboratory, Oak Ridge, TN, 2003.
[11] T. Hylton, G. Bastiaans, E. Daymo, T. Thomas, Comparative Testing of Pipeline Slurry Monitors, Report No. DOE/EM-0490, Oak Ridge National Laboratory, Oak Ridge, Tennessee, 1999.
[12] J. Lowe, D. Koestler, J. Stevens, C. Burrows, K. Cooper, A. Gonzalez, G. Harrop, E. Lahoda, M. Levenson, A. Leviton, P. Mulik, A. Pezone, R. Varrin, Comprehensive Review of the Hanford Waste Treatment Plant Flowsheet and Throughput, Report no., US Department of Energy Office of Environmental Management, Washington, DC, 2006
[13] M. Mazzola, M. Grothaus, M. Walch, J. Jones-Meehan, M. Halpin, B. Little, J. Johnsone, New electrical control methods to prevent power plant fouling, in: Proceedings of the 1994 Technology Transfer Conference, Fossil Operations, Baton Rouge, LA, 1994.
[14] M. Morris, L.-L. JL, B. Lewis, Pipeline Unplugging Assessment and Recommendations for the Fernald Environmental Management Project, Report no., Oak Ridge National Laboratory, 2004
[15] J. Paddock, S. Mustafiz, M. Islam, A new technique for cleaning horizontal wellbores, Petrol Sci. Technol. 24 (2006) 807–819.
[16] M. Powell, Initial Actr Retrieval Technology Evaluation Test Material Recommendations, Report no., Pacific Northwest National Lab., Richland, WA, 1996
[17] M. Powell, G. Golcar, J. Geeting, Retrieval Process Development and Enhancements Waste Simulant Compositions and Defensibility, Report no., Pacific Northwest Lab., Richland, WA, 1997
[18] V. Raju, A Transport Study of Sodium Phosphate Dodecahydrate Pipeline Plugging Mechanisms, Ph.D. thesis, Mississippi State University, 2001.
[19] D. Smith, B. Olson, Double-shell Tanks System Maintenance and Recovery Needs Report, Report no., CH2MHill Hanford Group, Inc., Richland, WA, 2002
[20] D. Wiggert, R. Otwell, F. Hatfield, The effect of elbow restraint on pressure transients, J. Fluid Eng T ASME 107 (1985) 402–406.
[21] D. Wood, S. Chao, Effect of pipeline junctions on water hammer surges, Transp. Eng J ASCE 97 (3) (1971) 441–457.
[22] E. Wylie, V. Streeter, Fluid Transients, McGraw-Hill International Book Co., New York, 1978.

[23] W. Zollinger, F. Carney, Pipeline blockage unplugging and locating equipment, in: Proceedings of the ANS 10th International Topical Meeting On Robotics And Remote Systems For Hazardous Environments, Gainesville, FL, 2004.

Appendix II. Notation

a: wave propagation velocity
A: pipe cross-sectional area
$\overline{d}$: mean particle diameter
D: pipe diameter
f: friction factor
g: gravitational acceleration
$\overline{G}$: mean pressure amplification factor
H: hydraulic-grade-line elevation
L: pipeline length
N: total number of unplugging cycles
P_v: Vent pressure
P_{vac}: vacuum level
Q: flow rate
T_s: suction time
T_d: drive time
T_v: vent time
V: flow velocity
τ_s: Shear strength
ρ: density